Origin of the plasma scalds in dielectric coatings induced by 1ω laser

Hu Wang, Hongji Qi, Jiaoling Zhao, Bin Wang, Yingjie Chai, Zhen Yu, and Jianda Shao

Citation: Appl. Phys. Lett. **108**, 141603 (2016); doi: 10.1063/1.4945687
View online: https://doi.org/10.1063/1.4945687
View Table of Contents: http://aip.scitation.org/toc/apl/108/14
Published by the American Institute of Physics

Origin of the plasma scalds in dielectric coatings induced by 1ω laser

Hu Wang,[1,2] Hongji Qi,[1,a)] Jiaoling Zhao,[1,2] Bin Wang,[1,2] Yingjie Chai,[1,2] Zhen Yu,[1,2] and Jianda Shao[1,b)]
[1]*Key Laboratory of Materials for High Power Laser, Shanghai Institute of Optics and Fine Mechanics, No. 390 Qinghe Road, Jiading District, Shanghai 201800, People's Republic of China*
[2]*University of Chinese Academy of Sciences, Beijing 100049, People's Republic of China*

(Received 4 February 2016; accepted 27 March 2016; published online 5 April 2016)

The plasma scalds initiated by a 1053 nm (1ω) nanosecond laser are separated from the defect-induced damage pits, which is verified as a result of the ionization wavefront with the subnanosecond laser. Considering the beam reflection from solid-state absorption fronts during the damage process, a theoretical scalding threshold about 6.84 J/cm^2 (12 ns) based on the energy required to start an air avalanche is evaluated and agrees well with the experimental scalding threshold. The occurrence order of the initial explosion and subsequent ionization wavefront is verified to explain most of the damage morphologies caused by the 1ω laser. In addition to the significance in laser conditioning or cleaning for a high-power laser system, the results also indicate that through the occurrence of plasma scalds it is possible to mark the onset time of air plasma during laser-coating interaction. © *2016 AIP Publishing LLC*. [http://dx.doi.org/10.1063/1.4945687]

Dielectric coatings are widely used as specific components to control the beam temporally or spatially in a high power laser system and generally processed by laser conditioning to improve the laser-induced damage threshold.[1–3] When irradiated by the 1053 nm (1ω) nanosecond laser, plasma scalds on the capping layer of dielectric coatings are characterized by surface discoloration due to the light scattering from nanoscale pin-holes within the scalding surface.[4] The coverage percentage of plasma scalds on the surface of optics is a crucial factor affecting the performance of optics through beam modulation or light scattering. Therefore, the plasma scalds may induce serious damage on downstream optics or weaken transmissive fluence.[5,6] The typical morphology of the plasma scalds was first reported by Genin and Stolz,[7] and then characterized in detail by our group.[4] The occurrence of plasma scalds has been widely recognized as the typical damage morphology of 1ω pulse in air and has continued to attract many researchers in recent years.[8–12] However, the fundamental physical mechanism by which laser-coating interaction leads to the plasma scalds on the capping layer is still obscure. The aim of this work is to reveal the origin of the plasma scalds in dielectric coatings induced by a 1ω laser.

Depending on the laser intensity and pulse-duration, the dimension of the plasma scalds is as high as several hundred micrometers. High resolution damage morphologies show one or more defect-induced damage pits in the center of the plasma scalds.[4] Such pits are generally related to nodular ejection in dielectric mirrors. Recently, pits induced by the non-visible absorbing defects or surface contaminants are also reported to be surrounded with plasma scalds.[9,11] Such interesting results imply that the occurrence of plasma scalds is insensitive to the detailed defect categories but to the physical processes after the stimulation of defect. Moreover, the shape of the plasma scalds show a similar dependence on the laser fluence and beam incidence as that of the damage ring patterns on the rear surface of fused silica.[4,13] The damage ring patterns were explained by Chambonneau *et al.* with a two-stage model involving the explosion of the defect and subsequent expansion of the ionization wavefront in air.[13,14] The plasma issued from the initial explosion provides the prerequisite priming electrons for starting the electron avalanche in air during the pulse. Based on the ionization wavefront, the absence of the damage ring patterns under a 351 nm (3ω) laser is also explained according to the energy required to ionize the neutral species. Coincidentally, few plasma scalds have been reported for the 3ω laser. Due to the extreme similarity on many aspects, we hypothesize that the two-stage model is also reasonable for the formation of plasma scalds.

A recent study on vacuum damage indicates that the surrounding air plays the role of catalyst for the ring formation mechanism.[15] Nevertheless, the damage ring patterns still appear on the flat substrate due to the lateral expansion of the ionization wavefront. Vacuum experiments for dielectric coatings depicted a more complicated damage phenomenon due to the sensitivity of coating properties and organic pollutants in our previous work.[16] Other studies also illustrated the influence of atmosphere on laser damage morphology in vaccum.[10] The above vacuum experiments have tried to study the damage morphologies by controlling the number density of neutral species that finally affect the formation and expansion of the ionization wavefront. In fact, separating the damage ring patterns or plasma scalds from defect-induced damage pits is the most direct evidence to illustrate the role of ionization wavefront on the final damage morphology. Although most vacuum experiments have weakened but not totally eliminated the damage ring patterns or plasma scalds, other complicated damage phenomena occur due to many unintentional factors of environment. In this work, we try to use a subnanosecond 1ω laser to separate the expansion process of the ionization wavefront from the defect-induced explosion. For this duration, defect-induced damage is still the major damage mechanism of dielectric

a)Electronic mail: qhj@siom.ac.cn
b)Electronic mail: jdshao@mail.shcnc.ac.cn

coatings, but the onset of the explosion process is much later than the duration. The separation of the ionization wavefront is in the temporal scale and the less unintentional factors are imported when comparing with the vacuum experiments.

The hafnia (545 nm) and silica (570 nm) layers and the hafnia/silica 1ω mirrors are fabricated on fused silica substrates with an electron-beam evaporation method. The values in parentheses depict the physical thickness. The laser damage test apparatus to irradiate the two single layers and mirrors were both detailed in Ref. 17. The 10 Hz, 1ω laser of 0.263 ns pulse duration (Full Width at Half Maximum, (FWHM)) is used to normally focus on the coating surface with a quartz lens to a spot diameter 384 μm ($\sim e^{-2}$). For comparison, another 10 Hz, 1ω laser of 12 ns pulse-duration (FWHM) with a spot diameter 553 μm ($\sim e^{-2}$) is also applied to irradiate samples.

To illustrate the plasma scalds with the 12 ns irradiation, the damage sites are examined by the field emission scanning electron microscope (FE-SEM, Zeiss Auriga S40). Only the local scalding regions surrounding the damage pits are shown in Fig. 1. The outer scalding region is not shown and is similar to that of the shown regions. The surface of hafnia is burned more severely than that of silica under similar fluence. There are a variety of shapes for the damage pits in the center of plasma scalds, which result from different damage mechanisms. The flat-bottom-pit in Figs. 1(a) and 1(c) is due to the local interface fracture or poor adhesion at the hafnia-substrate interface. The shallow pit in Fig. 1(b) is related to the initiator close to the coating surface. The small digs in Figs. 1(d) and 1(h) are related to the thermal effect caused by the nanoabsorbing defects. Most of the damage pits on silica present the asteroid cracks and are similar to the surface damage of fused silica, which indicates the processes such as thermal explosion and shockwave, as shown in the Figs. 1(e)–1(g). The scalding phenomenon is absent when the fluence is close to 7 J/cm^2 for both coatings, as shown in Figs. 1(a) and 1(e). The earlier study indicated that the surface entrance damage characteristics are due to thermal shock from the hot plasma contiguous to the surface.[18] Explosive boiling occurs much more easily on the coating surface than bulk material due to the porous structure which facilitates the bubble nucleation. However, the formation mechanism of the hot plasma that is in a large area within the pulse duration is still unclear.

Damage caused by the defects, such as nodular defects, polishing defects, external contaminants, and nonstoichiometric defects in the nanosecond region, is well recognized by most researchers, and the damage pits are mainly related to the explosion of various defects. Expansion and ablation of the irradiated material are the major processes during the explosion, which is a relatively slow process due to the transport of heavy particles. Generally, the typical timescale of ablation is on the order of nanosecond.[19] According to the hypothesis, the plasma issued from the initial explosion provides the prerequisite priming electrons for starting an electron avalanche in air during the laser pulse. If the pulse duration is larger than the timescale of the explosion, the ionization wavefront formed strongly absorbs the remaining pulse and propagates with a very high speed. The temperature of the ionization wavefront is very high and behaves as the hot plasma. As reported in Ref. 20, the energy acquired by free electrons during laser pulse cannot be in excess of

$$E_m = \frac{Me^2 I}{2\epsilon_0 c m_e^2 \omega^2}, \tag{1}$$

where M is the average mass of air atoms/molecules, e is the electron charge, I is the laser intensity, ϵ_0 is the vacuum permittivity, c is the speed of light in vacuum, m_e is the electron mass, and ω is the laser frequency. The typical ionization energy of neutral species in air is about 12 eV. According to Eq. (1), the laser intensity required to reach the ionization energy is about 2.14 GW/cm^2 (i.e., threshold intensity) at 1ω. For the 12 ns Gaussian pulse, the corresponding threshold fluence is about 27.34 J/cm^2 according to $F = 0.5\sqrt{\pi/\ln 2 I\tau}$, where F is the incident fluence and τ is the pulse-duration. However, from Fig. 1, it is very obvious that plasma scalds appear on the coatings when the incident fluence is much below the threshold fluence. According to Figs. 1(a) and 1(e), the threshold fluence for the formation of

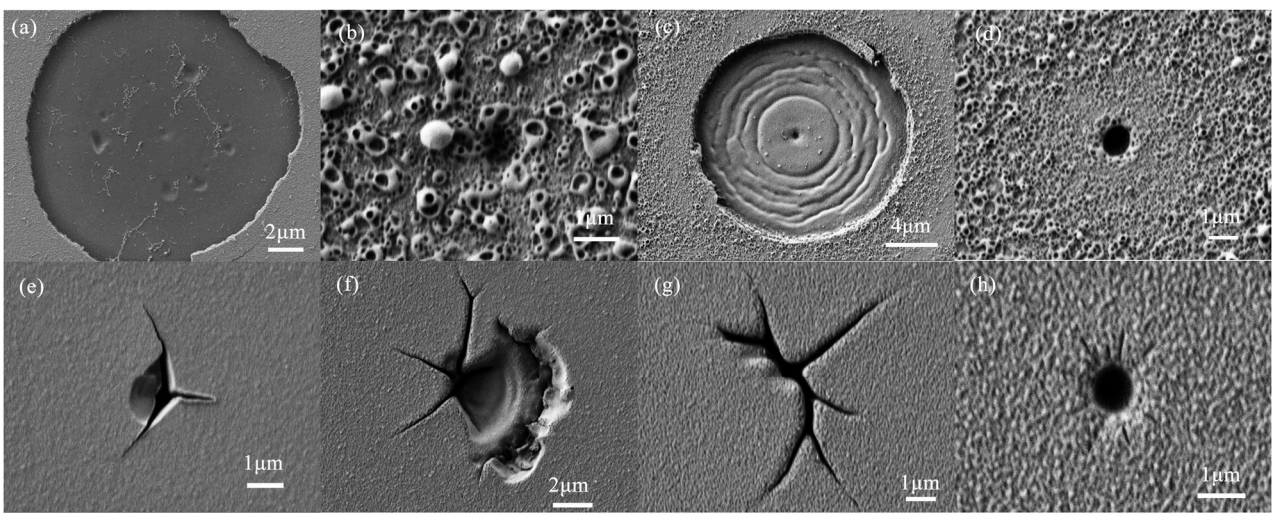

FIG. 1. SEM morphologies of the plasma scalds surrounding the pits for the hafnia under fluences: (a) 7 J/cm^2, (b) 10.7 J/cm^2, (c) 17.5 J/cm^2, (d) 20.5 J/cm^2, and for silica under fluences: (e) 6.9 J/cm^2, (f) 10.3 J/cm^2, (g) 13.7 J/cm^2, (h) 20.5 J/cm^2.

plasma scalds should be close to 7 J/cm^2 (denoted as experimental scalding threshold), which is in contrast to the resulting theoretical fluence evaluated as Eq. (1).

During the damage process, the initial defect is strongly heated by the laser and the surrounding transparent matrix is transferred into an absorptive state (by band-gap collapse, conduction, and radiation)[21] when it surpasses the critical temperature. The formed laser-supported solid-state absorption fronts in solids strongly absorb and reflect the laser beam.[22] At the strongly absorptive state, the reflectivity of absorption fronts tends to 1 and the maximal laser intensity in air shows about a fourfold rise,[18] which is independent on the detailed coating material. Therefore, we infer that the required incident fluence to start the electron avalanche in air would decrease to a quarter of 27.34 J/cm^2 (i.e., 6.84 J/cm^2, the scalding threshold fluence). Considering the reflection during the damage process, the evaluated scalding threshold fluence agrees well with the experimental scalding thresholds.

According to the study of material response during nanosecond laser induced breakdown,[23] the onset of electronic excitation in the solid is less than 1 ns, while the onset and growth of cracks is about 3 ns. The plasma inside the solid ejects out through the formed cracks and behaves as the prerequisite priming electrons to start an electron avalanche in air. To separate the ionization wavefront in air from the initial explosion, we apply the 1ω subnanosecond laser to excite the material. Under the 0.263 ns irradiation, there is not enough time for the plasma in the solid to eject out before the pulse is over. Although the laser intensity of the 0.263 ns laser in the air is much higher than that of the 12 ns laser, it is hard for the 0.263 ns laser to form an ionization wavefront due to a lack of the prerequisite priming electrons. The damage morphologies of the coatings under the 0.263 ns laser are shown in Fig. 2. The scalding phenomenon for all the coatings and different fluences is not observed, but the damage pits related to the defects still exist. As shown in Figs. 2(a) and 2(b), the presented damage pits are similar to those induced by the 12 ns laser in Fig. 1, which indicates the similar initiators for both lasers. The damage morphologies for mirrors irradiated by both lasers are shown in Figs. 2(c) and 2(d), respectively. The damage pits are similar, but the plasma scalds are missing for the 0.263 ns laser. The suppression of plasma scalds indicates that the escaping time of the plasma in solids is much longer than 0.263 ns, and the formation of plasma scalds is related to the propagation of the ionization wavefront. The experimental results here verify the importance of the ionization wavefront on the plasma scalds in our hypothesis. Although the redeposition of ejections was proposed to be responsible for the formation of plasma scalds,[4] the plasma scalds are not observed for the 0.263 ns laser. For the shorter pulse, the redeposition process can still happen later, which cannot support the absence of the plasma scalds.

To further reveal the two-stage mechanism, the damage pits for both lasers are studied with the focused ion beam (FIB) module equipped inside the SEM. Comparing Fig. 3(a) with Fig. 3(b), we found that the appearance of plasma scalds is like a scalding skin covering the coatings and damage pits. Similar morphologies are also observed for the mirrors in Figs. 3(c) and 3(d). The plasma scalds are separated from the damage pits while keeping the similar damage pits available. The results indicate that the defect behaves as a switch for initiating the explosion, which determines the damage threshold of coatings. However, the breakdown process of air due to the interaction between the remaining laser and electrons ejecting from the explosion will be responsible for the final scalding phenomenon. In addition, the scalding structures deposited on the sidewalls of damage pits verify the order of occurrence of the initial explosion and subsequent ionization wavefront.

With the verified order of occurrence of explosion and subsequent scalds, we can explain most of the observed damage morphologies caused by the 1ω 12 ns laser. In addition to the initial explosion, the scalding process can also remove some materials due to the thermal shock of hot plasma. The final damage morphology near the damage pit is the superposition of explosion depth and scalding depth. Generally, the explosion depth is dependent on the bury depth of the defect,

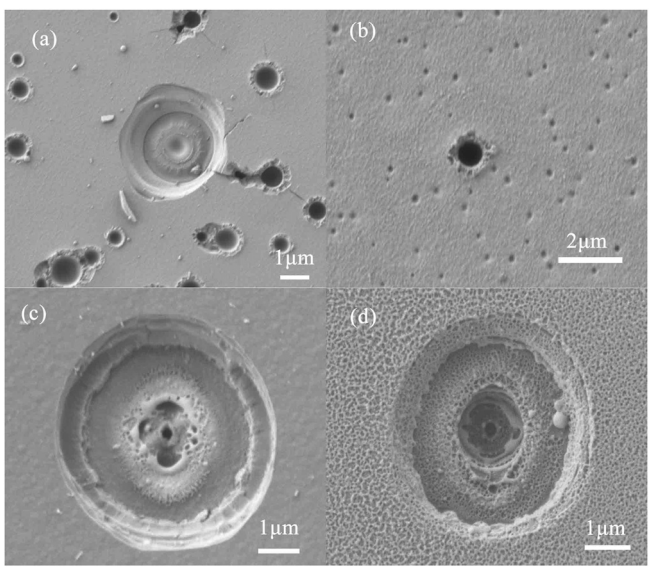

FIG. 2. SEM morphologies of damage sites for 0.263 ns laser under fluences: (a) 15.3 J/cm^2 (silica), (b) 13.6 J/cm^2 (hafnia), (c) 33.0 J/cm^2 (mirror), and for 12 ns laser under fluences: (d) 55.5 J/cm^2 (mirror).

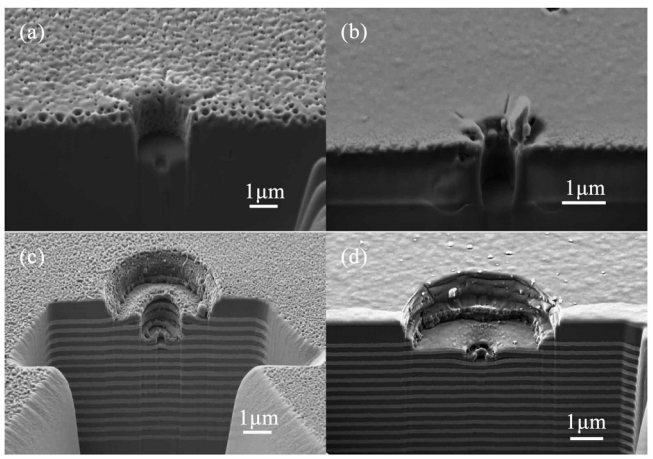

FIG. 3. FIB cross-section of the damage pits for silica under fluences: (a) 20.5 J/cm^2 (12 ns), (b) 10.3 J/cm^2 (0.263 ns), and for mirror under fluences: (c) 55.5 J/cm^2 (12 ns), (d) 18.2 J/cm^2 (0.263 ns).

while the scalding depth is dependent on the laser fluence.[4] The scalding depth is limited to one hundred nanometers and far less than the explosion depth in most cases. Therefore, most of the damage morphologies are the plasma scalds surrounding damage pits, such as in Figs. 1(c), 1(d), and 1(f)–1(h). The shape of the damage pits is mainly dependent on the detailed defect categories and explosion process. However, there is a rarely but really existing case in which the defect is buried closed to the coating surface. In such a case, the explosion depth might be totally covered by scalding depth, and the damage pit in the center of the plasma scalds is hard to observe. A similar case can be possible for the surface contaminants. Nevertheless, an undiscoverable damage pit can be observed with the high resolution SEM, as shown in Fig. 1(b). Generally, such a damage phenomenon mainly happened on the hafnia coatings or the capping layer consisting of hafnia, prepared by either the electron beam evaporation or ion beam sputtering method.

In summary, we verify the hypothesis to reveal the origin of plasma scalds by separating the ionization wavefront from defect induced damage pits with a subnanosecond laser. Considering the beam reflection due to solid-state absorption fronts during the damage process, a theoretical scalding threshold about 6.84 J/cm^2 is evaluated and agrees well with the experimental scalding threshold. The formation of plasma scalds is found to be closely related to ionization wavefront in air. By verifying the order of occurrence of the initial explosion and subsequent scalds, various damage morphologies caused by the 1ω laser can be explained, even for the shallow defects or surface contaminants. The coverage percentage of plasma scalds has always been an important assessment index during the laser conditioning for a high-power laser system. Recently, the damage phenomenon due to surface contaminants on the optics for a high-power laser system has been reviewed,[11] and the laser cleaning is an important method to eliminate the contaminants.[12] Decreasing the expansion time of the ionization wavefront is beneficial to weaken the interaction between the ionization wavefront and the pulse tail. Therefore, the coverage percentage of plasma scalds is reduced, and the performance of laser conditioning or cleaning can be improved with the shorter 1ω pulse duration (from nanosecond to subnanosecond). Moreover, our results indicate that the plasma scalds in dielectric coatings may be applied to mark the onset time of air plasma during laser-coating interactions by adjusting the laser duration.

The authors wish to express their gratitude to Zhou Fang for his experimental work. This work was supported by the Chinese National Natural Science Foundation (Grant No. 61308021) and the International Science and Technology Cooperation Program of China (2012DFG51590).

[1]J. Lindl, O. Landen, J. Edwards, E. Moses, and N. Team, Phys. Plasmas **21**, 020501 (2014).
[2]L. M. Sheehan, M. R. Kozlowski, and R. J. Tench, Proc. SPIE **2633**, 457–463 (1995).
[3]C. J. Stolz, L. M. Sheehan, S. M. Maricle, S. Schwartz, M. R. Kozlowski, R. T. Jennings, and J. Hue, Proc. SPIE **3264**, 105–112 (1998).
[4]X. Liu, Y. Zhao, D. Li, G. Hu, Y. Gao, Z. Fan, and J. Shao, Appl. Opt. **50**, 4226–4231 (2011).
[5]J. Schmidt, M. Runkel, K. Martin, and C. Stolz, Proc. SPIE **6720**, 67201H (2007).
[6]H. Wang, H. Qi, M. Guo, Y. Chai, B. Wang, K. Yi, and J. Shao, Opt. Lett. **40**, 2925–2928 (2015).
[7]F. Y. Genin and C. J. Stolz, Proc. SPIE **2870**, 439–448 (1996).
[8]J. Yao, J. Ma, C. Xiu, Z. Fan, Y. Jin, Y. Zhao, H. He, J. Shao, H. Huang, F. Zhang, and Z. Wu, J. Appl. Phys. **103**, 083103 (2008).
[9]W. Sun, H. Qi, Z. Fang, Z. Yu, Y. Liu, K. Yi, and J. Shao, Opt. Express **22**, 2948–2954 (2014).
[10]Y. Pu, P. Ma, S. Chen, J. Zhu, G. Wang, F. Pan, P. Sun, X. Zhu, J. Zhu, and D. Xiao, J. Appl. Phys. **112**, 023111 (2012).
[11]S. R. Qiu, M. A. Norton, R. N. Raman, A. M. Rubenchik, C. D. Boley, A. Rigatti, P. B. Mirkarimi, C. J. Stolz, and M. J. Matthews, Appl. Opt. **54**, 8607–8616 (2015).
[12]C. D. Harris, N. Shen, A. M. Rubenchik, S. G. Demos, and M. J. Matthews, Opt. Lett. **40**, 5212–5215 (2015).
[13]M. Chambonneau, P. Grua, J.-L. Rullier, J.-Y. Natoli, and L. Lamaignère, J. Appl. Phys. **117**, 103101 (2015).
[14]M. Chambonneau, R. Diaz, P. Grua, J.-L. Rullier, G. Duchateau, J.-Y. Natoli, and L. Lamaignère, Appl. Phys. Lett. **104**, 021121 (2014).
[15]R. Diaz, M. Chambonneau, P. Grua, J.-L. Rullier, J.-Y. Natoli, and L. Lamaignère, Appl. Surf. Sci. **362**, 290–296 (2016).
[16]X. Ling, Appl. Surf. Sci. **257**, 5601–5604 (2011).
[17]W. Liu, C. Wei, J. Wu, Z. Yu, H. Cui, K. Yi, and J. Shao, Opt. Express **21**, 22476–22487 (2013).
[18]N. Boling, G. Dub, and M. Crisp, Appl. Phys. Lett. **21**, 487–489 (1972).
[19]B. Rethfeld, K. Sokolowski-Tinten, D. von der Linde, and S. Anisimov, Appl. Phys. A **79**, 767–769 (2004).
[20]Y. B. ZelDovich and Y. P. Raizer, *Physics of Shock Waves and High-Temperature Hydrodynamic Phenomena* (Academic Press, New York, 1966), Vol. I, Chap. V.
[21]S. Papernov and A. Schmid, J. Appl. Phys. **97**, 114906 (2005).
[22]C. Carr, J. Bude, and P. DeMange, Phys. Rev. B **82**, 184304 (2010).
[23]S. G. Demos, R. A. Negres, R. N. Raman, A. M. Rubenchik, and M. D. Feit, Laser Photonics Rev. **7**, 444–452 (2013).